RSC Advances

ROYAL SOCIETY OF CHEMISTRY

www.rsc.org/advances

Journal Name

RSCPublishing

ARTICLE

Enhanced gas sensing performance of indium doped zinc oxide nanopowders

Cite this: DOI: 10.1039/x0xx00000x

Received 00th January 2012,
Accepted 00th January 2012

DOI: 10.1039/x0xx00000x

www.rsc.org/

David C. Pugh[a,b], Vandna Luthra[c], Anita Singh[c] and Ivan P. Parkin[b*]

A series of indium doped ZnO (IZO) materials were fabricated, characterised and tested for their gas sensing properties. ZnO was synthesised with indium doping levels of 0.2, 0.5, 1 and 3 mol %. These were fabricated into gas sensors. Production took place using a commercially available screen printer, a 3 × 3 mm alumina substrate containing interdigitated electrodes and a platinum heater track. Materials were characterised using X-ray diffraction (XRD), scanning electron microscopy (SEM) and energy dispersive X-ray spectroscopy (EDX). Electrical conductivity of all samples was also calculated. Sensors were exposed to ethanol, methanol, *n*-butanol and acetone at concentrations between 5 and 80 ppm. Low levels of indium doping were found to increase the responsiveness of the sensors. However, higher levels of doping were found to inhibit conductivity and responsiveness to gases of IZO sensors. Sensors with low levels of indium doping were found to show minimal response to other gases, demonstrating a lack of cross sensitivity. These sensors show potential for inclusion into an electronic nose for with the aim of selective alcohol detection.

[a] Department of Security and Crime Science, University College London, 35 Tavistock Square, London, WC1H
[b] Department of Chemistry, University College London, 20 Gordon Street, London, WC1H 0AJ, UK
[c] Department of Physics, Gargi College, Siri Fort Road, New Delhi, 110049, India

Journal Name RSCPublishing

ARTICLE

Introduction

Metal oxide semiconducting (MOS) gas sensors are a low cost and reliable method of vapour detection. Their ease of production, high robustness and simple interface electronics make them ideal candidates for commercial detection. MOS sensors operate on the principle that a change in conductivity of the material occurs on contact with an analyte gas.

The gas sensing properties of zinc oxide were first demonstrated 1962 by Seiyama *et.al.*[1] and the material has since been found to be a versatile gas sensing material that has been used on a number of devices, including sensor to detect carbon monoxide[2,3], hydrogen[4,5], nitrogen oxides[6,7], hydrocarbons[8,9], alcohols[10,11,12], ammonia[13,14,15] and disulphides[16]. The working temperature of ZnO gas sensors is generally quite high, around 300°C-500°C, and selectivity is generally poor. As a result of this, preparation methods and doping of ZnO gas sensors to reduce operating temperature and to increase the stability, sensitivity and selectivity of materials are major research topics[17,18].

A wide range of techniques have been employed to improve sensor responses and working conditions. These include the use of zeolites[1920], carbon nanotubes[21], nanoparticles[22] and doping of the material[23]. Each of these techniques has their own merits and faults. Metal-ion doping of MOS materials enhances the gas-sensing properties by changing energy-band structure and morphology[24], as well as increasing adsorption area and consequently creating more centers for gas interaction on the metal oxide semiconductor surface[25].

Electronic properties of ZnO solids can be tuned through the incorporation of various dopants, usually group 13 elements; Aluminum[26,27], Gallium[28] and Indium[29]. Doping ZnO materials with these materials replaces Zn^{2+} ions with higher valence M^{3+} ions, increasing impurities in the material.
A number of different doping techniques have been investigated, to produce both thick and thin film gas sensors. These include: co-sputtering[30], thermal evaporation[31], pulsed laser deposition[32] and ball milling[33].

In this study, indium doped zinc oxide (IZO) powders were synthesized, characterized and tested for the monitoring of low concentrations of gas in air. Doped and pure zinc oxide powders were prepared using a low cost, scalable co-precipitation technique. This is a robust and reliable technique, which is easy to implement, as it does not require any expensive or complex equipment. Co-precipitation techniques have been used to produce a wide range of gas sensing materials in previous investigations. [34,35,36].
To our knowledge, this is the first example of indium doping of ZnO, for thick film gas sensing purposes.
Ethanol (C_2H_5OH), which is a volatile, flammable, colourless liquid, is most commonly used as a solvent and in alcoholic beverages; however, it is also used as a fuel, an intoxicant and in thermometers.
Methanol (CH_3OH) is a highly toxic alcohol, often indistinguishable from ethanol on account of their similar appearance and odour. It is commonly used in the production of formaldehyde, and from there in the production of paint, plastics and plywood.
n-Butanol (C_4H_9OH) is a straight chained primary alcohol. It is primarily used as a solvent, chemical intermediate and as a paint thinner. It is also considered as a potential biofuel[37] as well as an additive to diesel in order to reduce soot emissions.
Acetone (C_3H_6O) is a flammable, colourless, mobile liquid, and a simple ketone. Acetone is a commonly used solvent for many plastics and synthetic fibres.

Experimental

Material Preparation

ZnO and indium doped ZnO were produced using a co-precipitation technique. For the production of pure ZnO, zinc acetate ($Zn(OAc)_2.2H_2O$), supplied by Sigma-Aldrich, was fully dissolved in methanol. Subsequently, a 0.5 M solution of NaOH was added drop wise over a period of 2 hours. The resulting precipitate was washed with ethanol and water and filtered. The precipitate was subsequently calcined at 700°C for 3 hours.

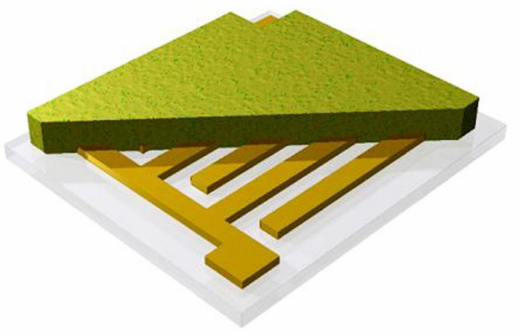

Figure 1 MOS film on alumina substrate, showing gold electrodes. The substrate is 3 x 3 mm with 0.15 mm between the interdigitated electrodes. Image courtesy of City Technology Ltd.

For the production of indium doped ZnO, indium nitrate ($In(NO_3)_3.xH_2O$, (Alfa Asear)) was used as a doping agent and dissolved with suitable quantities of zinc acetate. This produced In doped ZnO with 0.2, 0.5, 1 and 3 mol % Indium.

For electrical conductivity measurements, samples were pressed into pellets and silver paste was deposited onto both sides of each sample.

Device Fabrication

Materials were fabricated by printing ZnO and IZO inks onto 3 x 3 mm alumina substrate tiles, containing laser etched digitated electrodes and an integrated platinum heater track (electrode gap 0.15 mm, Fig.1). Inks were produced by mixing powders with an organic vehicle (ESL-400).

The inks were ground by pestle and mortar to produce a smooth, homogenous suspension. Screen-printing was performed on a DEK1202 printer. Ink was printed onto a strip of alumina substrates simultaneously. A total of 5 layers of ink were printed to the substrate (~75 µm thickness). Between applications, the ink was dried under an infra-red lamp for 20 minutes. Following application of all layers, individual sensors were fired for 1 hour at 600°C in an Elite thermal systems BRF15 furnace. The sensors were bonded onto brass pins in a standard poly-phenylene sulphide housing using platinum wire (0.0508 mm thickness, supplied by Alfa Aesar) and a MacGregor DC601 parallel gap resistance welder.

Characterisation Techniques

The sensors were characterised by X-ray Diffraction (XRD), Scanning Electron Microscopy (SEM) and Energy Dispersive X-ray (EDX) spectroscopy, before and after exposure to test gases. Diffraction patterns were collected over the 2θ range 10° to 75°, step size 0.02°, on a Brucker GADDS D8 diffractometer using Cu Ka radiation (λ = 0.15418 nm). Scanning electron micrographs were collected on a Jeol JSM- 6301F microscope, in secondary electron imaging mode, using a 5 keV probe voltage. The images were digitally recorded using SemAfore software. EDX analysis was performed using a 20 keV SEM probe coupled with an Oxford Instruments INCA X-Sight system and associated software, this confirmed the atomic percentage make up of each sample.

The dc conductivity of the undoped and doped ZnO pellets were measured at room temperature using a Keithely 2400 Source Meter.

Gas Sensing Experiments

Gas sensing experiments took place on an in-house testing rig[38]. The rig consists of a sensing chamber consisting of 12 sensor ports, connected to analytical standard gas supplies (supplied by BOC), controlled by three mass flow controllers. A potential divider circuit and an analog to digital converter card allow recording of resistance measurements.

The sensor array was initially exposed to 1200 seconds of dry air, to establish a baseline. This initial purge was followed by five gas pulses of 600 seconds each, interspersed with 1200 second air pulses, in order to allow the sensors to recover and re-establish a baseline. Sensors were exposed to ethanol and acetone (supplied by BOC) at concentrations of 5, 10, 20, 40 and 80 ppm, in ascending order. Wheatstone bridge circuits allowed the sensors operating temperatures to be independently set to 500 °C, 400 °C and 350 °C. Experiments were repeated in triplicate to ensure repeatability of the sensors.

Results and Discussion

X-ray diffraction patterns were collected for all samples (Fig. 2). All zinc oxide based materials show a predominant wurzite phase structure with high crystallinity, which can be matched with the Joint Committee on Powder Diffraction Standards (JCPDS card no. 36-1451) and literature studies on ZnO[39]. All samples display strong peaks at 2θ = 31.37°, 34.03°, 35.86°, 47.16°, 56.26° and 62.54°. No additional peaks were found in undoped ZnO. In indium doped ZnO, while the ZnO wurzite phase remains predominant, two low intensity peaks are observed (marked with *) showing the formation of an In_2O_3 corundum phase (JCPDS, No. 65,3170). The intensity of these peaks increases with increasing indium doping. These peaks are clearly visible in 1% and 3% IZO materials, in lower doped IZO and ZnO, the materials are single phased.

SEM images of the sensor surface were recorded at 50,000x magnification (Fig. 3) and show the porous nature of the materials. Figure 3.a shows ZnO with an average grain size of 120 nm. Fig 3.b Shows hexagonal grains approximately 140 nm in diameter. Fig 3.c displays hexagonal grains, with an average grain diameter of 145 nm. Fig 3.d shows IZO (1%) with grains displaying less hexagonal characteristic and larger in diameter

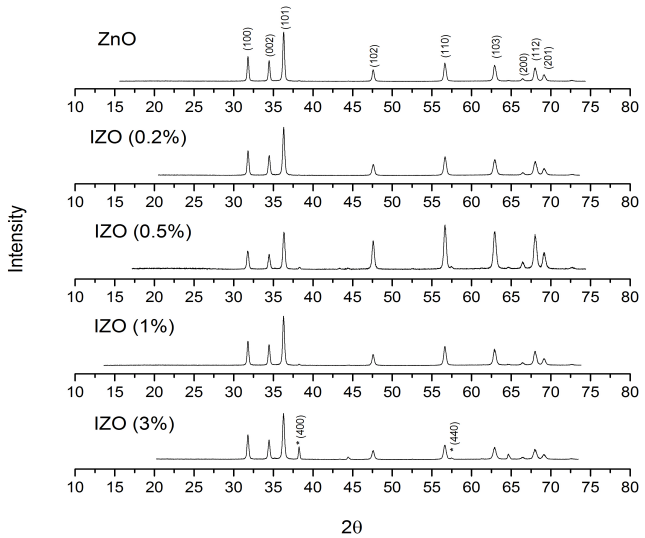

Figure 2 Diffraction patterns for ZnO and IZO sensors, collected between circa 10° and 75°. The y-axis is normalised and offset for each spectrum. Principle peaks are indexed according to their standards from the literature[36]

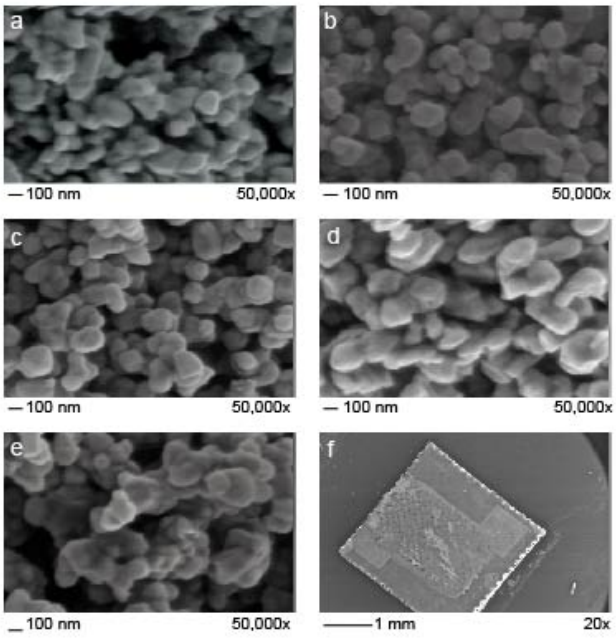

Figure 3 SEM micrographs for all sensor chips. All images are at 50,000x magnification. a) ZnO, b) IZO (0.2%), c) IZO (0.5%), d) IZO (1%), e) IZO (3%) f) Screen printed ZnO Sensor

approximately 200-250 nm. Fig 3.e shows IZO (3%) with larger fused grains around 180 nm in diameter. Fig 3.f shows a sensors substrate with printed metal oxide material, for reference. As indium content increases, the hexagonal characteristics of the material become more defined. However, above 0.5% doping, the material loses its hexagonal characteristic, and larger grains are formed.

EDX analysis showed consistent oxygen and zinc abundances, as well as the expected indium concentrations in all samples (Table 1). Multiple batches of ZnO and IZO powders were produced and analysed, showing variation in indium concentration was less that 0.2 %RSD in all samples.

Table 1 Atomic percentage of zinc, oxygen and indium in ZnO and IZO materials

	Atomic percentage		
	Zn	O	In
ZnO	53.0	47.0	0.0
IZO (0.2%)	52.7	46.9	0.21
IZO (0.5%)	52.4	46.5	0.51
IZO (1%)	52.0	46.9	0.90
IZO (3%)	50.0	47.1	2.90

Electrical properties

The conductivity of all samples was calculated from the linear region of I-V curves (fig. 4). The dc conductivity was calculated using the equation:

$$\sigma = \frac{t}{RA}$$

Where σ is the dc conductivity, t is the thickness, A is the area and R is the resistance of the samples, σ has the units: Ω^{-1} cm^{-1}.

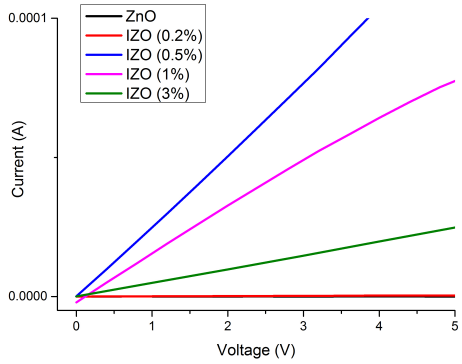

Figure 4 Variation in current with voltage at room temperature

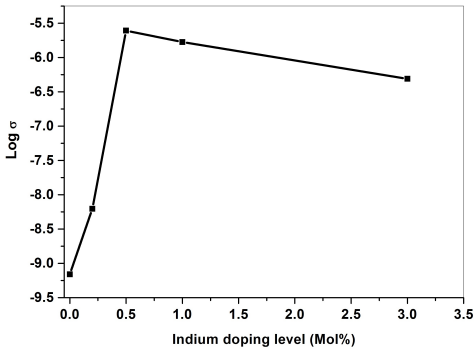

Figure 5 Variation in logσ with indium doping level

The magnitude of conductivity in indium-doped materials is higher than the unmodified ZnO. This increase can be explained by two reasons: firstly the increase in electron– hole pairs leads to an increase in carrier concentration as a result of indium incorporation[40]. Secondly a large increase in the dopant concentration causes the formation of a degenerate semi-conductor with high conductivity. The increased carrier concentration in the degenerate semiconductor can also lead to metallic behaviour of the In-doped ZnO[41].

In IZO materials with 1% and 3% indium, the conductivity starts to decrease again. This decrease can be explained by the high dopant concentration increasing the probability of the ionized impurity centre scattering charge carriers, which can influence the electronic mobility, reducing the conductivity

This may also have contributed to the fusing of grains observed in Fig.3[42].

The effects of metal impurities on the electrical conductivity of ZnO have been studied in great detail. Many researchers propose that dopants could enhance the excess oxygen concentration in the grain boundary region of the material and form a potential barrier preferentially[43,44]. Therefore, the electrical conductivity of the In doped ZnO samples is apparently higher than that of the undoped ZnO, and the grain boundary is more resistive than the grain. Conductivity increases with increasing indium concentration, to 0.5%, and then reduces; this reduction in the conductivity is thought to be due to the inactivity of added dopant atoms and the formation of a minor In_2O_3 as well as other morphological changes phase.

Gas sensing results

Gas sensing responses are shown as a function of their baseline resistance (R_0/R). R_0 is the baseline resistance, calculated as the average resistance prior to the first gas pulse. An example of the results obtains can be seen in Fig. 6.

Strong conductive responses (decreases in resistance) to ethanol vapour were found at all temperatures. Indium doped sensors

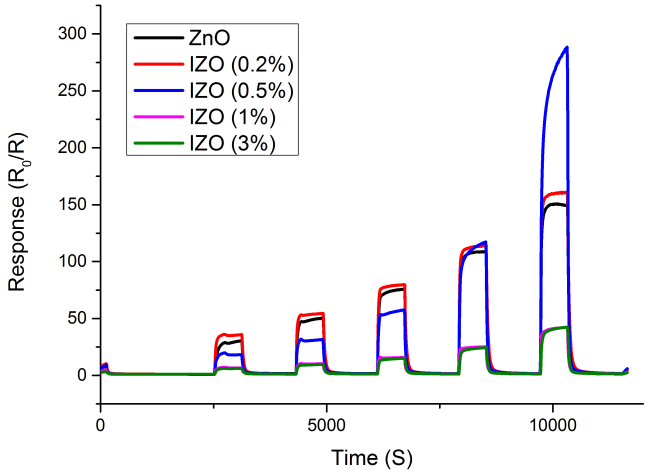

Figure 6 Response to 5 ZnO and IZO sensors, exposed to 600 s pulses of 5, 10, 20, 40 and 80 ppm of ethanol at 400°C in dry air

show a larger magnitude of response as compared with the unmodified ZnO sensor. The magnitude of response in IZO sensors doped with 0.2 % and 0.5 % indium were significantly larger than unmodified ZnO with 0.5 % doping being the most responsive. IZO sensors with 1 and 3 % In doping showed much lower responses than both undoped ZnO and IZO materials with lower doping levels, a likely result of their lower conductivity. All sensors showed a larger magnitude of conductive response, at higher gas concentrations, due to the increased availability of ethanol in the environment to react at the sensor surface.

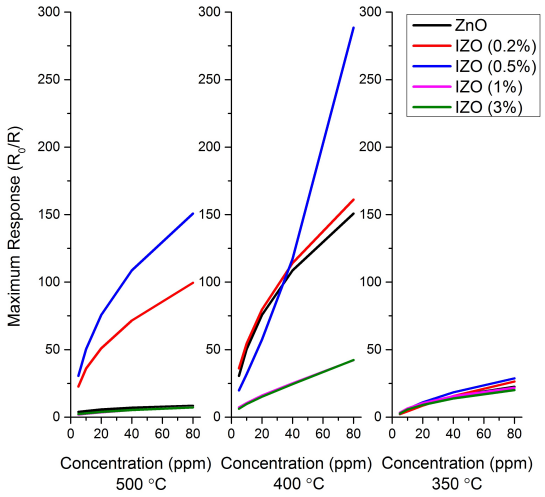

Figure 7 Maximum responses of all sensors to ethanol at concentrations between 5-80 ppm in a 600 s exposure

Indium doped ZnO samples with low doping levels show a marked increase in their responsiveness to gasses at [illegible] temperatures (Fig.7). It is commonly known that the sensing mechanism in MOS based sensors is surface controlled. The surface microstructure, grain size, oxygen adsorption and surface states all play a key role in the sensor performance. Responses in all sensors were shown to be of the highest magnitude at 400°C. Plots of the maximum response to ethanol vapour against temperature are not linear, but show plateauing effects in most cases, suggesting that these sensors world be best suited to detection of concentrations of ethanol less that 100 ppm, as sensors may become saturated at higher concentrations. The exception to this is IZO (0.5%), which shows an almost exponential increase.

All sensors were exposed to three successive pulses of 40 ppm ethanol. Results from this experiment (Fig.8) show good repeatability between sensors, with the magnitude of response between these three pulses and a 40-ppm pulse in fig 6 in agreement. Additionally, the peak shape between all pulses is similar, as are the response and recovery times.

This three pulse test was repeated for IZO (0.5% at 400 °C), 1 week, 1 month, 3 months and 6 months after the first exposures to ethanol, in order to monitor the long term stability issues often experiences by MOS gas sensing materials. The average response of these tests has been recorded (Fig. 9) and shows limited variation over a 6 month time period, with a standard deviation of 2.02 and a relative standard deviation of 1.78 %.

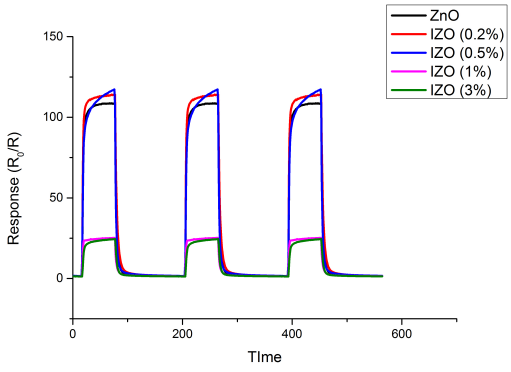

Figure 8 Gas sensing response of all samples to three successive pulses of 40 ppm ethanol

Table 2 Response time of ZnO and IZO sensors, upon exposure to various concentrations of ethanol at 400 °C

Concentration (ppm)	Response Time (S, ±5)				
	ZnO	IZO (0.2%)	IZO (0.5%)	IZO (1%)	IZO (3%)
5	120	70	80	80	80
10	80	50	60	50	50
20	70	50	40	50	60
40	60	40	40	30	60
80	50	40	50	40	60

Table 3 Recovery time of ZnO and IZO sensors, following exposure to various concentrations of ethanol at 400 °C

Concentration (ppm)	Recovery Time (S, ±5)				
	ZnO	IZO (0.2%)	IZO (0.5%)	IZO (1%)	IZO (3%)
5	90	80	50	80	80
10	90	90	70	100	90
20	80	100	90	100	100
40	80	100	100	100	110
80	90	110	100	100	110

The sensor response time (τ_{Res}), is the time taken to reach 90% of the maximum response value, upon exposure to a particular concentration of gas. The recovery time (τ_{Rec}), is the time taken for a sensor to reach within 10% of its original baseline, following a gas pulse[45].

The response time (Table 2) and recovery Time (table 3) at 400°C are displayed. The response time of all sensors decrease with increasing concentration. This is because at higher concentrations, more ethanol is available for reaction at the sensor surface and so the rate of reaction at the sensor surface will increase. The response time of doped ZnO sensors is generally less that that of pure ZnO, despite low doped sensors displaying higher response values. All IZO sensors display response times within 20 seconds of each other.

Recovery times (Table 3) following exposure to various ethanol concentrations are found to increase with increasing ethanol concentration, this is a result of having a greater concentration of ethanol adsorbed on the sensor surface. Recovery times for IZO sensors are also found to be generally higher than for the pure ZnO sensor.

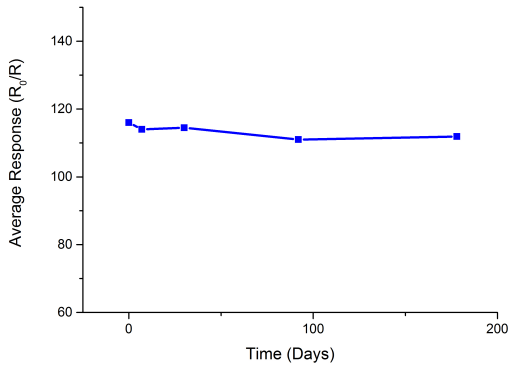

Figure 9 Response of IZO (0.5%) to 40 ppm ethanol over a 6 month period

Sensors were subsequently exposed to *n*-butanol, under the same experimental conditions as when exposed to ethanol (Fig 10). Once again, IZO sensors were found to increase the responsiveness to the analyte gas, in the same order, that is IZO (0.2%) and IZO (0.5%) sensors were found to have the largest responses. The magnitude of response for IZO sensors when exposed to n-butanol, as opposed to ethanol, indicates that the functional groups of an analyte gas are not the only factor in determining a gas response, with stoichiometric, kinetic and thermodynamic properties being important factors in predicting a gas sensor response, in addition to structural properties.

Upon exposure to methanol, again, under the same experimental conditions as previously demonstrated (Fig 11), low doped IZO sensors were found to give enhancement over pure ZnO, with IZO sensors that were doped with more indium showing responses of similar magnitude to undoped ZnO. The magnitude of response for methanol was found to besignifficantly lower than that of ethanol in all sensors, at all operating temperatures, with the largest magnitude of response found to be 3.41, for IZO (0.5%) to 80 ppm of ethanol at 400°C.

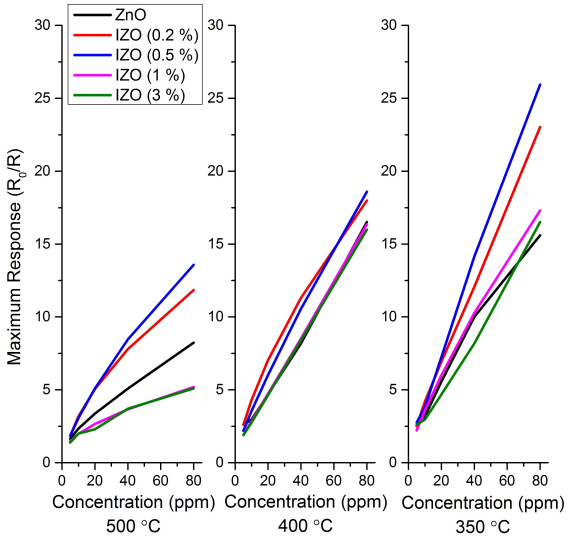

Figure 10 Maximum responses of all sensors to *n*-butanol at concentrations between 5-80 ppm in a 600 s exposure

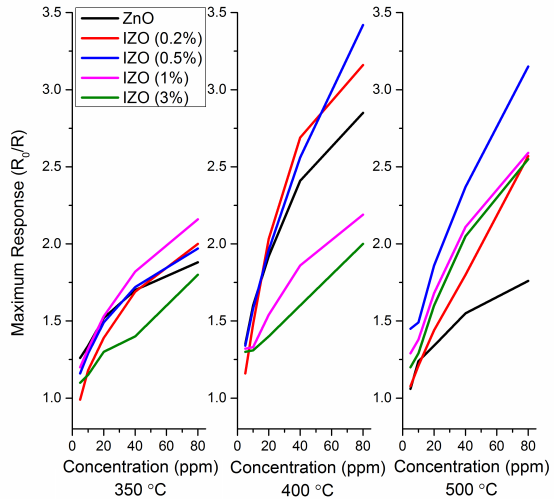

Figure 11 Sensor responses to methanol at concentrations between 5 and 80 ppm at 500, 400 and 350°C in dry air for a 600 s exposure

Sensors were also exposed to the same concentrations of acetone, under the same experimental conditions. The results of these exposures (Fig.12) are found to be much smaller in magnitude than those of ethanol exposure. The relative order of responses are the same as that of ethanol exposure, with 0.2 % and 0.5 % indium doped samples showing large enhancements, while 3 % indium doped sensor shows very poor response to acetone (R_0/R <2).

The sensors response to ethanol is far superior to the responses displayed upon exposure to a number of other gases at the same operating temperature and concentrations (Fig. 11). In light of these results, Indium doped ZnO, with 0.5 % indium doping shows great promise for inclusion into gas sensing array with the purpose of detecting ethanol.

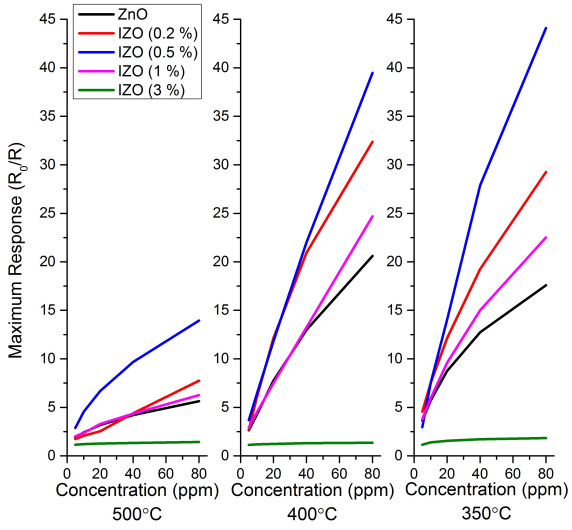

Figure 12 Sensor responses to acetone at concentrations between 5 and 80 ppm at 500, 400 and 350°C in dry air for a 600 s exposure

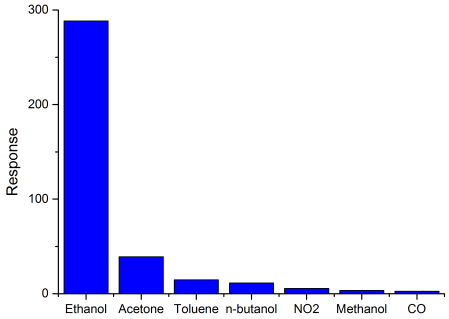

Figure 13 Response of IZO (0.5%) to a variety of gases at 40 ppm and an operating temperature of 400°C

Mechanism

Initially, at elevated temperatures, oxygen species are adsorbed onto the surface, forming $O_{(ads)}^-$ species and removing electrons from the material, this leads to the formation of a depleti region. In the presence of a reducing gas (R), oxygen is removed from the surface, reintroducing trapped electrons into the material, decreasing the size of the depletion region and increasing the conductivity. This can be generally described as:

$$O_{2(g)} + 2e^- \rightarrow 2O^-_{(ads)}$$

$$R_{(g)} + O^-_{(ads)} \rightarrow RO_{(g)} + e^-$$

Doping In^{3+} in the place on Zn^{2+} increases the conductivity of the material, due to increased electron density. Therefore indium doping facilitates the creation of $O^-_{(ads)}$ species and electrons are more readily available at the sensor surface. It is well known that the responsiveness of gas sensors relates directly to the number of $O^-_{(ads)}$ species at the sensor surface[46]. With increased conductivity in indium-doped materials, more $O^-_{(ads)}$ species are formed, meaning a larger change in magnitude is possible as there are more positions for reducing gases to react at the sensor surface.

However, too much doping will lead to the screening effect induced by the surface doped ion aggregation, which is unfavourable to the gas diffusion into the sensing films, leading a decrease in the responsiveness of sensors[40,47].

Different magnitudes of response are observed at different operating temperatures. There are a number of reasons for this. The adsorption and desorption of oxygen and analyte gasses, which control the baseline resistance and magnitude of gas response, are greatly affected by the surface temperature of t sensor, residence time on the sensor surface is partly determined by the temperature and reactions at the surface occurring too fast or slow can lead to detrimental effects on t sensor response. Physical properties of the material such as; Debye length, work function and charge carrier concentration are also affected by the temperature. These sensors show go d levels of reproducibility, with all results showing less than 3% variation in identical tests.

To all gases tested, IZO samples with 1 and 3% doping show poor results, this is attributed to a combination of the decrease in conductivity, the formation of a secondary In_2O_3 phase and to changes in the microstructure and agglomeration of grains in higher doped samples.

Undoped ZnO responses are consistent with studies both from our laboratory[48] and others[49]. Indium doped ZnO of 0.5% was found to be the most responsive, with a response of R_0/R = 288.4 to 80 ppm of ethanol. Low doping levels of Indium in ZnO materials show larger responses to similar concentrations of ethanol than SnO_2[50], Fe_2O_3[51] and WO_3[52].

Conclusions

A series of ZnO and indium doped ZnO sensors were synthesised and manufactured. This is, to our knowledge, the first example of thick films IZO materials being used for ethanol vapour detection. Low doping levels of indium in zinc oxide showed an increase in the responsiveness to ethanol (from R_0/R = 150 to R_0/R = 288), methanol (from R_0/R= 90 to R_0/R= 191) and acetone (from R_0/R = 17.5 to R_0/R = 44.1). Post exposure characterisation of the sensor materials found that neither heating of the sensors nor exposure to gases caused any structural change to the materials. This material stability combined with long-term exposure tests to IZO materials suggests strong robustness over a long time period. The ease of production of materials and sensors, combined with the low cost of synthesis materials and sensor electronics mean that these materials show great potential for low cost, highly sensitive ethanol sensors.

Acknowledgments

Authors wish to thank Dr. Steve Firth, Martin Vickers and Dr Tom Gregory for assistance in technical matters relating to the study. This work was carried out under a UGC-UKIERI Thematic Partnership Grant 2013.

[1] T. Seiyama, A. Kato, K. Fujiishi, and M. Nagatani. *Analytical Chemistry, 1962,* **34**, 1502.
[2] J.H. Yu and G.M. Choi, *Sensors and Actuators B*, 1999, **61**, 59.
[3] B. Bott, T. A. Jones, and B. Mann, *Sensors and Actuators*, 1984, **5**, 65.
[4] M. Egashira, N. Kanehara, Y. Shimizu, and H. Iwanaga, *Sensors and Actuators*, 1989, **18**, 349.
[5] S. Saito, M. Miyayama, K. Koumoto, and H. Yanagida, *Journal of the American Ceramic Soc*iety, 1985, **68**, 40.
[6] R. Lambrich, W. Hagen, and J. Logois, *Analytical Chemistry Symposium Series,* 1983, **17**, 73.
[7] P. Romppainen, V. Lantto, and S. Leppavuori, *Sensors and Actuators B*, 1990, **1**, 73.
[8] C. N. R. Rao, A. R. Raju, and K. Vijayamohanan, Gas-Sensor Materials, in New Materials (S. K. Joshi, T. Tsuruta, C. N. R. Rao, and S. Nagakura, Eds., Narosa, New Delhi, 1992, and the references therein).
[9] G.Williams and G. S.V. Coles, *Sensors and Actuators B*, 1999, **57**, 108.
[10] B. P. J. d. L. Costello, R. J. Ewen, N. M. Ratcliffe, and P. S. Sivanand, *Sensors and Actuators B*, 2003, **92**, 159.
[11] A. R. Raju and C. N. R. Rao, *Sensors and Actuators B*, 1991, **3**, 305.
[12] B.P. de Lacy Costello, R.J. Ewen, N. Guernion, N.M. Ratcliffe, *Sensors and Actuators B*, 2002, **87**, 207.
[13] M. Egashira, Y. Shimizu, and Y. Takao, *Sensors and Actuators B*, 1990, **1**, 108.
[14] H. Nanto, T. Minami, and S. Takata, *Journal of Applied Physics*, 1986, **60**, 482.
[15] M.S. Wagh, G.H. Jain, D.R. Patil, S.A. Patil, *Sensors and Actuators B* 2006, **115**, 128.
[16] B. P. J. d. L. Costello, R. J. Ewen, P. R. H. Jones, N. M. Ratcliffe, and R. K. M.Wat, *Sensors and Actuators B*, 1999, **61**, 199.
[17] X. Lou, *Journal of Sensor and Transistor Technology,* 1991, **3**, 1.
[18] X.LCheng, H. Zhao, L. H. Huo, S. Gao, and J. G. Zhao. *Sensors and Actuators B,* 2004, **102**, 248.
[19] P.T Hernández, A.J.T. Naik, E.J. Newton, S.M.V. Hailes and I.P.Parkin, *Journal of Materials Chemistry A*, 2014, **23**, 8952.
[20] D.C. Pugh, S.M.V. Hailes and I.P. Parkin, *Measurement Science and Technology,* 2015, In press
[21] G.P. Evans, D.J. Buckley, N.T. Skipper, and I.P. Parkin, *RSC Advances,* 2014, **93**, 51395.
[22] W.J. Peveler, R. Binions, S.M.V. Hailes and I.P. Parkin. *Journal of Materials Chemistry A*, 2013, **1**, 2613.

[23] S.T. Shishiyanu, T.S. Shishiyanu and O.I. Lupan. *Sensors and Actuators B: Chemical*, 2005, **107**, 379.
[24] M. Hjiri, L. El Mir, S.G. Leonardi, A. Pistone, L. Mavilia and G. Neri, *Sensors and Actuators B*, 2014 **196**, 413.
[25] M. Hjiri, R. Dhahri, K. Omri, L. El Mir, S.G. Leonardi, N. Donato, G. Neri, *Materials Science in Semiconductor Processing* 2014 **27** 319.
[26] S. Ghosh, A. Sarkar, S. Chaudhuri, A.K. Pal, *Thin Solid Films*, 2005, **205**, 605. ,
[27] Anita and V. Luthra. *Ceramics International*, 2014, **40**, 14927
[28] X. Yu, J. Ma, F. Ji, Y. Wang, C. Cheng and H. Ma, *Applied Surface Science*, 2005, **245**, 310.
[29] P.M. Ratheesh Kumar, C. Sudha Kartha, K.P. Vijayakumar, T. Abe, Y. Kashiwaba, F. Singh, D.K. Avasthi, *Semiconductor Science and Technol*ogy, 2005, **20**, 120.
[30] H. Gong, Hu J.Q., Wang, J.H., Ong, C.H. and Zhu F.R. *Sensors and Actuators B, 2006,* **115**, 247.
[31] A Khanna, *Applied Physics Literature, 2003,* **82**, 4388.
[32] I.G. Dimitrov, A.Og. Dikovska, P.A. Atansov, T.R. Stoyanchov, T. Vasilev, *Journal of Physics: Conference Series,* 2008, **113**, 012044
[33] M.H. Shahrokh Abadi, R. Wagiran, M.N. Hamidon, A.H. Shaari, N. Adbullah, N. Misron, and M. Malekzadeh. *International journal of engineering and technology, 2009, **6**,* 60.
[34] Meng, F., Yin, J., Duan, Y. Q., Yuan, Z. H., & Bie, L. J. *Sensors and Actuators B*, 2011, **156**, 703.
[35] C. Xiangfeng, *Materials research bulletin*, 2003, **38**, 1705.
[36] Z. Sun, L. Lang, Z.J. Dian and W. Pan. *Sensors and Actuators B,* 2007, **1**, 144.
[37] D. Antoni, V. Zverlov, and W.H. Schwarz, *Applied Microbiology and Biotechnology*, 2007, **77**, 23.
[38] S.C. Naisbitt, K.F.E. Pratt, D.W. Williams, and I.P. Parkin, *Sensors and Actuators B*, 2006, **114**, 969.
[39] J.L.Van Heerden, & R. Swanepoel, *Thin Solid Films*, 1997, ***299***, 72.
[40] K. Ellmer and R. Mientus. *Thin solid films*, 2008, **516**, 4620.
[41] J.M. Phillips, R.J. Cava, G.A. Thomas, S. A. Carter, J Kwo, T. Siegrist, J. J. Krajewski, J. H. Marshall, W. F. Peck Jr and D.H. Rapkine, Applied physics letters, 1995, **67,** 2246.
[42] V.Luthra, K.F.E. Pratt, R.G. Palgrave, D.E. Williams, R.P. Tandon, and I. P. Parkin *Polyhedron* 2010, **29,** 1225.
[43] N. Ohashi, Y. Terada, T. Ohgaki, S. Tanaka, T. Tsurumi, O. Fukunage, H. Haneda, J. Tanaka, *Japanese journal of applied physics*. 1999, **38** 5028.
[44] F. Oba, I. Tanaka, H. Adachi, *Japanese journal of applied physics*. 1999, **38**, 3569.
[45] C. Liewhiran and S. Phanichphant *Sensors,* 2007, **7**, 185.
[46] K Zakrzewska. *Vacuum*, 2004, ***74***, 335.
[47] R. K. Sharma, M. C. Bhatnagar, and G. L. Sharma, *Sensors and Actuators B,* 1997, **45**, 209.
[48] D.C.Pugh, E.J. Newton, A.J.T Naik, S.M.V. Hailes and I.P. Parkin *Journal of Materials Chemistry A*, 2014, **2**, 4758.
[49] M. Kalyan Chakravarthi and B. Bharath, in Mechatronics and its Applications (ISMA), 2012 8th International Symposium, IEEE, 2012, p. 1. 50
[50] T. Jinkawa, G. Sakai, J. Tamaki, N Miura, and N. Yamazoe. *Journal of Molecular Catalysis A: Chemical*, 2000, **155**, 193.
[51] Y. Wang, J. Cao, S. Wang, X. Guo, J. Zhang, H. Xia, and S. Wu. *The Journal of Physical Chemistry C*, 2008. **112**, 17804.
[52] R.S. Khadayate, R.B. Waghulde, M.G. Wankhede, J.V. Sali, and P.P. Patil, *Bulletin of Materials Science*, 2007, **30**, 129.